Sensitized Near-Infrared Emission from Complexes of Yb^{III}, Nd^{III} and Er^{III} by Energy-Transfer from Covalently Attached Pt^{II}-Based Antenna Units

Nail M. Shavaleev,[a] Lucy P. Moorcraft,[a] Simon J. A. Pope,[b] Zöe R. Bell,[a] Stephen Faulkner,*[b] and Michael D. Ward*[a]

Abstract: A series of dinuclear platinum(II)–lanthanide(III) complexes has been prepared in which a square-planar Pt^{II} unit, either $[(PPh_3)_2Pt(pdo)]$ (H_2pdo = 5,6-dihydroxyphenanthroline) or $[Cl_2Pt(dppz)]$ [dppz = 2,3-bis(2-pyridyl)pyrazine], is connected to a $\{Ln(dik)_3\}$ unit ("dik" = a 1,3-diketonate ligand). The mononuclear complexes $[(PPh_3)_2Pt(pdo)]$ and $[Cl_2Pt(dppz)]$ both have external, vacant N,N-donor diimine-type binding sites that react with various $[Ln(dik)_3(H_2O)_2]$ units to give complexes $[(PPh_3)_2Pt(\mu\text{-}pdo)Ln(tta)_3]$ (series **A**; Htta = thenoyltrifluoroacetone), $[Cl_2Pt(\mu\text{-}dppz)Ln(tta)_3]$ (series **B**); and $[Cl_2Pt(\mu\text{-}dppz)Ln(btfa)_3]$ (series **C**; Hbtfa = benzoyltrifluoroacetone); in all of these the lanthanide centres are eight-coordinate. The lanthanides used exhibit near-infrared luminescence (Nd, Yb, Er). Crystal structures of members of each series are described. In all complexes, excitation into the Pt-centred absorption band (at 520 nm for series **A** complexes; 440 nm for series **B** and **C** complexes) results in characteristic near-IR luminescence from the Nd, Yb or Er centres in both the solid state and in CH_2Cl_2, following energy-transfer from the Pt antenna chromophore. This work demonstrates how d-block-derived chromophores, with their intense and tunable electronic transitions, can be used as sensitisers to achieve near-infrared luminescence from lanthanides in suitably designed heterodinuclear complexes based on simple bridging ligands.

Keywords: dinuclear complexes · energy transfer · lanthanides · luminescence · N ligands · platinum

Introduction

The intense, long-lived and line-like emission from the lanthanide ions Eu^{III} and Tb^{III} has made their compounds of intense interest for a wide range of applications such as display devices, luminescent sensors and probes for clinical use (e.g., fluoroimmunoassay).[1] In contrast, the longer-wavelength luminescence from other lanthanides such as Yb^{III}, Nd^{III} and Er^{III}, which occurs in the near-infrared (NIR) region, has only relatively recently become of interest,[2–7] and the development and exploitation of NIR luminescence in lanthanide complexes lags a long way behind that of Eu^{III} and Tb^{III} complexes.

Although NIR luminescence is weak compared to that from Eu^{III} and Tb^{III}, it is of considerable technological significance in two quite different fields. Firstly, it could be exploited for medical-imaging purposes, because of the relative transparency of human tissue in the NIR region. The use of a NIR luminophore would not only allow the radiation emitted from an in vivo probe to be detected outside the body, but would also allow more penetrating long-wavelength light to be used for excitation. What makes the use of NIR-emitting lanthanides in this way particularly appealing is that many of the major problems of ligand design, kinetic and thermodynamic stability of complexes, and their biocompatibility and biodistribution have already been solved during the development of Gd^{III} complexes as MRI contrast enhancement agents.[8]

The second important application of NIR luminescence from lanthanides is in optical telecommunications systems that are based on silica fibres. Silica has windows of transparency at ca. 1330 and 1550 nm, which are the wavelengths used for optical data transmission. Some attenuation still occurs and is compensated for by amplifiers that boost the signal; these amplifiers contain Pr^{III} and Er^{III}, whose emission wavelengths are, conveniently, at wavelengths that are close to the transparency windows of silica.[9]

The very weak (Laporte forbidden) and narrow f–f transitions of lanthanides[10] means that direct excitation requires intense (laser) sources at precise wavelengths. It is far more common and convenient to stimulate luminescence by exploiting energy-transfer from a ligand that contains

[a] Prof. M. D. Ward, Dr. N. M. Shavaleev, L. P. Moorcraft, Dr. Z. R. Bell
School of Chemistry, University of Bristol
Cantock's Close, Bristol BS8 1TS (UK)
Fax: (+44) 117-929-0509
E-mail: m.d.ward@sheffield.ac.uk

[b] Dr. S. Faulkner, Dr. S. J. A. Pope
Department of Chemistry, University of Manchester
Oxford Road, Manchester M13 9PL (UK)
Fax: (+44) 161-275-4598
E-mail: stephen.faulkner@man.ac.uk

 DOI: 10.1002/chem.200305132

suitable strongly absorbing aromatic chromophores such as pyridyl or phenyl groups.[2–7] Whilst excitation of aromatic ligands in the UV/blue region, which is necessary with Eu^{III} and Tb^{III}, can certainly be used to stimulate NIR emission from other lanthanides, it would be useful—for the reasons given above—to be able to use longer wavelength (visible/red) excitation. Therefore, complexes of Er^{III}, Nd^{III}, and so forth need to be designed that contain suitable chromophores for excitation at these wavelengths.

One approach to this is to use as ligands suitably functionalised organic dyes that have particularly low-energy $\pi-\pi^*$ transitions. By using chromophores such as fluorenone dyes[5] or tetrazine[4] in the ligands, sensitised emission from NIR-emitting lanthanides has been observed using excitation wavelengths of 500–550 nm. A potentially more versatile approach, which is the subject of this paper, is to exploit strongly absorbing transition-metal chromophores as antenna groups to achieve sensitised NIR emission from lanthanides. There are clear advantages to this approach. Transition-metal complexes can have very strong charge-transfer absorptions, at a range of wavelengths that span the visible region, with extinction coefficients of the order of $10^4\ M^{-1}\ cm^{-1}$. In many series of complexes the relationship between ligand substituents and absorption spectrum is well understood, such that "fine tuning" of the absorption maximum is straightforward.

To exploit the strong light-absorbing properties of d-block complexes as antenna groups in this way in molecular species, preparation of heterodinuclear complexes is required in which the d-block antenna unit is connected to the f-block NIR luminophore unit by a short bridging ligand that will allow effective $d \rightarrow f$ energy transfer to occur. Examples of this in molecular species are rare, because they are based on highly asymmetric bridging ligands that have different binding sites for the d-block and f-block centres; this complicates the syntheses and means that the examples known are limited and far from generally applicable to a wide range of antenna/luminophore combinations. Thus various workers have used metalloporphyrins as the antenna group to achieve sensitised NIR emission from lanthanides;[11] van Veggel and co-workers have used both ferrocenyl and $[Ru(bpy)_3]^{2+}$ units as chromophores in a similar way.[12] Piguet and co-workers observed $f \rightarrow d$ $Eu^{III} \rightarrow Cr^{III}$ energy transfer, resulting in sensitised emission from Cr^{III} in a heterodinuclear Eu^{III}/Cr^{III} triple helicate,[13a] and sensitisation of lanthanide emission with Cr^{III} as energy-donor occurs in oxalato-bridged dinuclear complexes.[13b] The field of heterodinuclear d/f block assemblies and the properties that can arise from metal–metal interactions has recently been reviewed.[14]

We have recently developed a simple, stepwise method which allows a wide range of d-block chromophores to be attached to $\{Ln(dik)_3\}$ luminophores ("dik" = a 1,3-diketonate anion; Ln denotes a generic lanthanide ion) using the "complexes as ligands" approach.[15, 16] By using potentially bridging ligands, such as bipyrimidine, a kinetically inert d-block metal chromophore can be attached to one site, leaving the second N,N-donor site free. Attachment of a $\{Ln(dik)_3\}$ unit to the vacant N,N-donor site of the d-block "complex ligand" is facile and just requires reaction of the complex ligand with the appropriate $[Ln(dik)_3(H_2O)_2]$ in a non-polar solvent. The resulting adducts have high enough stability constants to remain largely associated in non-polar solvents, allowing $d \rightarrow f$ energy transfer to occur, resulting in sensitised luminescence from the lanthanide.[16] In this paper we describe how this method can be used to prepare a series of dinuclear Pt–lanthanide complexes, in which a $\{Pt(PPh_3)_2(catecholate)\}$ or $\{PtCl_2(diimine)\}$ unit (as chromophore) is connected to a $\{Ln(dik)_3\}$ NIR-emitting luminophore. The crystal structures of several dinuclear complexes of this type have been determined, and we show how excitation of the Pt-based chromophore using visible light results in sensitised NIR emission from the lanthanide unit in each case. A preliminary communication based on part of this work has been published recently.[16]

Results and Discussion

Synthesis and characterisation of complexes: The two d-block "complex ligands" used are $[(PPh_3)_2Pt(pdo)]$, in which a $\{Pt(PPh_3)_2\}^{2+}$ unit is coordinated to the diolate site of 5,6-dihydroxyphenanthroline (H_2pdo) and the phenanthroline site is free,[17] and $[Cl_2Pt(dppz)]$, in which one of the binding sites of a 2,3-di(2-pyridyl)pyrazine-bridging ligand is occupied by a $\{PtCl_2\}$ fragment and the other site is vacant;[18] these are known compounds.[17, 18] Reaction of these with a variety of

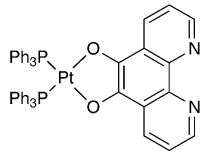

$[(PPh_3)_2Pt(pdo)]$

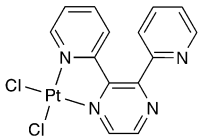

$[Cl_2Pt(dppz)]$

$[Ln(dik)_3(H_2O)_2]$ species in CH_2Cl_2/heptane or benzene/heptane afforded the dinuclear adducts by displacement of two water ligands from the coordination sphere of the lanthanide by the vacant N,N-donor site of the complex ligand. This synthesis is based on the well-known formation of eight-coordinate adducts between $\{Ln(dik)_3\}$ units and N,N-bidentate chelates such as 2,2′-bipyridine (bpy) or 1,10-phenanthroline (phen).[19] We note that use of $[(PPh_3)_2Pt(pdo)]$ as a "bipyridine equivalent" in this way for the formation of heterodinuclear (d–d) complexes has been described by others.[20]

The complexes prepared fall into three series: series **A**: $[(PPh_3)_2Pt(\mu\text{-pdo})Ln(tta)_3]$ (Htta = thenoyltrifluoroacetone), series **B**: $[Cl_2Pt(\mu\text{-dppz})Ln(tta)_3]$, and series **C**: $[Cl_2Pt(\mu\text{-dppz})Ln(btfa)_3]$ (Hbtfa = benzoyltrifluoroacetone). For simplicity, the complexes will be referred to by the series label and the lanthanide, for example, $[Cl_2Pt(\mu\text{-dppz})Yb(tta)_3]$ will be referred to as Yb(**B**) and so on. All complexes are air- and moisture-stable crystalline solids and were satisfactorily characterised on the basis of elemental analyses and some X-ray crystal structures. Whereas the series **A** and **C** complexes are highly soluble in CH_2Cl_2, the series **B** complexes were much less soluble; this prevented full photo-

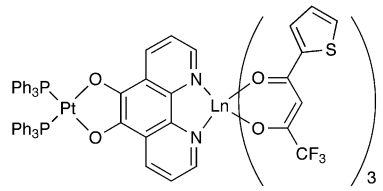

Series **A** complexes (Ln = La, Nd, Gd, Yb, Er)

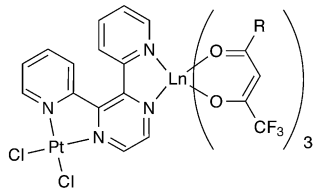

R = 2-thienyl; series **B** complexes (Ln = Nd, Gd, Er, Yb)

R = Ph; series **C** complexes (Ln = Nd, Er, Yb)

physical characterisation in solution (see later). The crystal structures of representative complexes of each series are shown in Figures 1–3 below; isostructural analogues for the series **A** complexes are not shown, but their details are included in the crystallographic tables.

The complexes Yb(**A**), Er(**A**), La(**A**) and Gd(**A**) are isostructural; the structure of Er(**A**) is shown in Figure 1 [the structure of Gd(**A**) was described in the earlier communication[16] and is not reproduced here]. The Pt^{II} centre is square

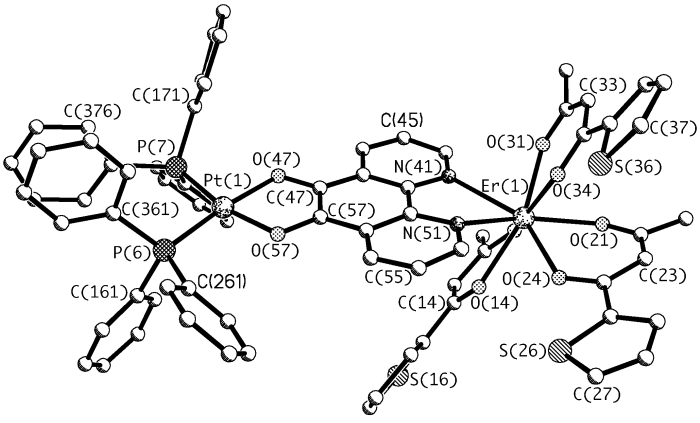

Figure 1. Molecular structure of $[(PPh_3)_2Pt(\mu\text{-pdo})Er(tta)_3]\cdot 0.5C_6H_6$ (solvent and F atoms omitted for clarity). The disorder between S(16) and C(19) is not shown.

planar; the eight-coordinate Er^{III} centre has an approximate square-antiprismatic geometry, with the two square planes consisting of atoms N(41)/N(51)/O(31)/O(34) and O(11)/O(21)/O(14)/O(24) Bond lengths and angles around individual metal centres are unremarkable. The Pt···Er distance is 8.38 Å. Selected bond lengths and angles for the series **A** complexes are collected in Table 1; the bond lengths around the various lanthanides follow the pattern expected on the basis of the lanthanide contraction. The bulky PPh_3 ligands

Table 1. Selected bond lengths [Å] and angles [°] for the series **A** complexes.

$[(PPh_3)_2Pt(\mu\text{-pdo})Er(tta)_3]\cdot 0.5\,C_6H_6$ [Er(**A**)$\cdot 0.5\,C_6H_6$]			
Er(1)–O(11)	2.287(7)	Er(1)–N(41)	2.499(7)
Er(1)–O(31)	2.300(7)	Er(1)–N(51)	2.522(8)
Er(1)–O(21)	2.304(6)	Pt(1)–O(57)	2.021(6)
Er(1)–O(14)	2.320(7)	Pt(1)–O(47)	2.040(6)
Er(1)–O(34)	2.322(8)	Pt(1)–P(6)	2.238(2)
Er(1)–O(24)	2.326(6)	Pt(1)–P(7)	2.241(2)
Er(1)···Pt(1)	8.381(1)		
O(57)-Pt(1)-O(47)	82.9(2)	O(57)-Pt(1)-P(7)	167.99(18)
O(57)-Pt(1)-P(6)	92.63(17)	O(47)-Pt(1)-P(7)	86.14(16)
O(47)-Pt(1)-P(6)	174.36(18)	P(6)-Pt(1)-P(7)	98.57(8)
$[(PPh_3)_2Pt(\mu\text{-pdo})La(tta)_3]$ [La(**A**)]			
La(1)–O(31)	2.440(9)	La(1)–N(41)	2.661(11)
La(1)–O(21)	2.455(9)	La(1)–N(51)	2.669(9)
La(1)–O(34)	2.479(9)	Pt(1)–O(57)	2.016(8)
La(1)–O(11)	2.479(9)	Pt(1)–O(47)	2.041(7)
La(1)–O(14)	2.487(10)	Pt(1)–P(6)	2.227(3)
La(1)–O(24)	2.497(8)	Pt(1)–P(7)	2.238(3)
La(1)···Pt(1)	8.543(2)		
O(57)-Pt(1)-O(47)	82.0(3)	O(57)-Pt(1)-P(7)	86.2(2)
O(57)-Pt(1)-P(6)	174.4(2)	O(47)-Pt(1)-P(7)	167.0(2)
O(47)-Pt(1)-P(6)	93.3(2)	P(6)-Pt(1)-P(7)	98.76(12)
$[(PPh_3)_2Pt(\mu\text{-pdo})Yb(tta)_3]$ [Yb(**A**)]			
Yb(1)-O(24)	2.268(11)	Yb(1)-N(51)	2.480(10)
Yb(1)-O(31)	2.273(10)	Yb(1)-N(41)	2.487(13)
Yb(1)-O(21)	2.304(11)	Pt(1)-O(47)	2.002(10)
Yb(1)-O(34)	2.310(10)	Pt(1)-O(57)	2.037(9)
Yb(1)-O(11)	2.313(11)	Pt(1)-P(6)	2.230(4)
Yb(1)-O(14)	2.326(11)	Pt(1)-P(7)	2.231(4)
Yb(1)···Pt(1)	8.345(2)		
O(47)-Pt(1)-O(57)	83.3(3)	O(47)-Pt(1)-P(6)	92.4(3)
O(57)-Pt(1)-P(6)	174.0(3)	O(57)-Pt(1)-P(7)	85.7(3)
P(6)-Pt(1)-P(7)	98.97(14)	O(47)-Pt(1)-P(7)	167.0(3)

preclude any axial Pt···Pt interactions between adjacent molecules.

The structure of Nd(**B**) is shown in Figure 2. Again, the Pt^{II} centre has the usual square-planar geometry, and the Nd^{III} centre is approximately square antiprismatic with the two sets

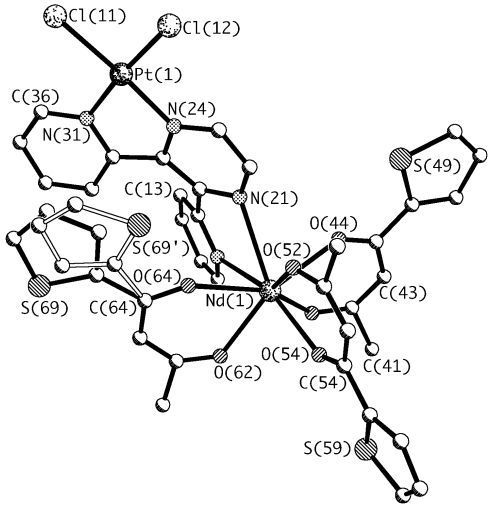

Figure 2. Molecular structure of $[Cl_2Pt(\mu\text{-dppz})Nd(tta)_3]\cdot CH_2Cl_2$ (solvent and F atoms omitted for clarity) including the disorder of one of the thiophene rings.

of four donors defining the planes being O(42)/(O44)/N(11)/N(21) and O(52)/O(54)/O(62)/O(64). The dppz bridging ligand has a rather distorted geometry, which is necessary to allow the two pyridyl rings to avoid another; the angles between the pyridyl rings and the central pyrazine ring are 39.3 and 14.7° for the pyridyl rings containing N(11) and N(31), respectively. The mean planes of the two pyridyl rings are at 49.9° to one another. The non-bonded Nd···Pt separation is 7.26 Å. Selected bond lengths and angles for this complex are in Table 2.

Table 2. Selected bond lengths [Å] and angles [°] for the series **B** and **C** complexes.

$[Cl_2Pt(\mu\text{-dppz})Nd(tta)_3]\cdot CH_2Cl_2$ [Nd(**B**)·CH_2Cl_2]			
Nd(1)–O(52)	2.368(9)	Nd(1)–N(11)	2.623(9)
Nd(1)–O(54)	2.371(7)	Nd(1)–N(21)	2.728(8)
Nd(1)–O(42)	2.377(8)	Pt(1)–N(24)	2.003(8)
Nd(1)–O(62)	2.401(8)	Pt(1)–N(31)	2.012(8)
Nd(1)–O(44)	2.410(9)	Pt(1)–Cl(12)	2.290(2)
Nd(1)–O(64)	2.463(12)	Pt(1)–Cl(11)	2.294(2)
Nd(1)···Pt(1)	7.220(1)		
N(31)-Pt(1)-Cl(12)	174.9(2)	N(24)-Pt(1)-Cl(11)	175.8(2)
N(24)-Pt(1)-N(31)	79.8(3)	N(31)-Pt(1)-Cl(11)	96.0(2)
N(24)-Pt(1)-Cl(12)	95.2(2)	Cl(12)-Pt(1)-Cl(11)	89.06(9)
$[Cl_2Pt(\mu\text{-dppz})Nd(btfa)_3]$ [Nd(**C**)]			
Nd(1)–O(61)	2.354(9)	Nd(1)–N(11)	2.655(9)
Nd(1)–O(41)	2.360(8)	Nd(1)–N(21)	2.700(9)
Nd(1)–O(63)	2.371(7)	Pt(1)–N(24)	1.973(10)
Nd(1)–O(51)	2.385(9)	Pt(1)–N(31)	2.009(9)
Nd(1)–O(53)	2.411(10)	Pt(1)–Cl(12)	2.295(3)
Nd(1)–O(43)	2.429(8)	Pt(1)–Cl(11)	2.301(3)
Nd(1)···Pt(1)	7.257(2)		
N(24)-Pt(1)-N(31)	79.5(4)	N(24)-Pt(1)-Cl(11)	175.9(3)
N(24)-Pt(1)-Cl(12)	95.5(3)	N(31)-Pt(1)-Cl(11)	96.4(3)
N(31)-Pt(1)-Cl(12)	175.0(3)	Cl(12)-Pt(1)-Cl(11)	88.59(11)

An interesting feature of this complex, which complicated the refinement, is the twofold disorder in the position of the thiophene ring that incorporates S(69) (see Figure 2). This ring lies stacked parallel to the planar $PtCl_2$(diimine) unit, with an average separation between the thiophene ring and the $PtCl_2N_2$ plane of about 3.5 Å, but has one of two different orientations with the S atom directed "inwards" or "outwards" with approximately equal likelihood. When this thiophene S atom is externally directed, it interacts with a fluorine atom from the CF_3 unit of an adjacent molecule (S(61)···F(61′), 2.70 Å). This distance is necessarily very approximate not only because of the disorder not only in the thiophene ring, but also due to the rotational disorder in the CF_3 groups; however, the fact that this contact is shorter than the sum of the van der Waals radii indicates an F···S donor–acceptor interaction. In addition, the absence of steric crowding around the open face of the planar $PtCl_2$(diimine) unit – -in contrast to the series **A** complexes—means that these planar units stack together, using the face that is not stacked with a thiophene unit, giving axial Pt···Pt contacts between adjacent molecules with a separation of 3.41 Å. This solid-state Pt···Pt interaction may account for the poor solubility of the series **B** complexes. The crystal structures of several other members of this series were determined, but the weakness of the data arising from disorder means that they are of poor quality and their details are not included in this paper; we just note that all of the investigated members of this series are isostructural with Nd(**B**).

The structure of Nd(**C**) is shown in Figure 3; again the complex contains essentially a square-planar Pt^{II} centre and square-antiprismatic Nd^{III} centres, with the two sets of four

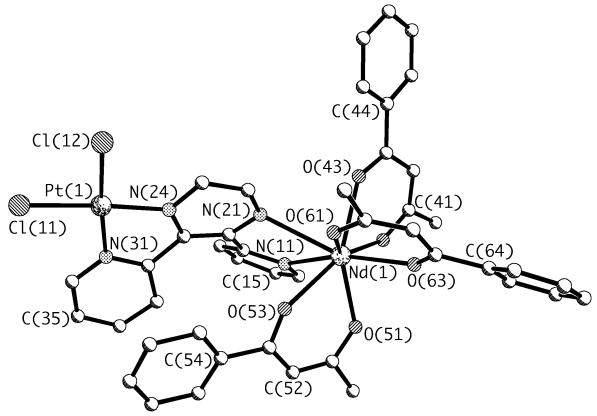

Figure 3. Molecular structure of $[Cl_2Pt(\mu\text{-dppz})Nd(btfa)_3]$. F atoms omitted for clarity.

donors defining the crude square planes around Nd(1) being O(51)/O(53)/O(61)/O(63) and N(11)/N(21)/O(41)/O(43). The dppz bridging ligand has a similar twisted geometry to that seen in Nd(**B**), with the mean planes of the pyridyl rings containing N(11) and N(31) making angles of 38.8 and 17.0°, respectively, with the mean plane of the pyrazine ring; the two pyridyl mean planes are at 53.3° to one another. The planar $PtCl_2N_2$ units of two adjacent molecules are stacked together across an inversion centre; these mean planes are therefore strictly parallel, with a separation of 3.34 Å and a Pt···Pt distance of 3.42 Å. The Pt(1)···Nd(1) separation within the complex molecule is 7.26 Å.

UV-visible spectra and stability constants in solution: For eight-coordinate complexes of the type $[Ln(dik)_3(NN)]$, there is a reversible equilibrium in solution involving association/dissociation of the NN-donor ligand.[4, 19c] When NN = 2,2′-bipyridine or 1,10-phenanthroline the association constant for Equation (1) is of the order of $10^7\ M^{-1}$ in hydrocarbon solvents[19c] and slightly less in more polar solvents such as CH_2Cl_2.

$$[Ln(dik)_3(H_2O)_2] + NN \rightleftharpoons [Ln(dik)_3(NN)] + 2H_2O \quad (1)$$

The association constant for this process was measured by a UV-visible spectroscopic titration for a member of each of the three series of complexes; this was achieved by adding increasing amounts of $[Ln(dik)_3(H_2O)_2]$ to a solution of the d-block complex ligand $[(PPh_3)_2Pt(pdo)]$ or $[Cl_2Pt(dppz)]$ in CH_2Cl_2 and monitoring the absorption spectral changes. Representative results are shown in Figure 4.

The absorption spectra of mononuclear $[(PPh_3)_2Pt(pdo)]$ and the $\{Gd(tta)_3\}$ adduct Gd(**A**) are shown in Figure 4a. $[(PPh_3)_2Pt(pdo)]$, which is orange-brown, has its lowest-

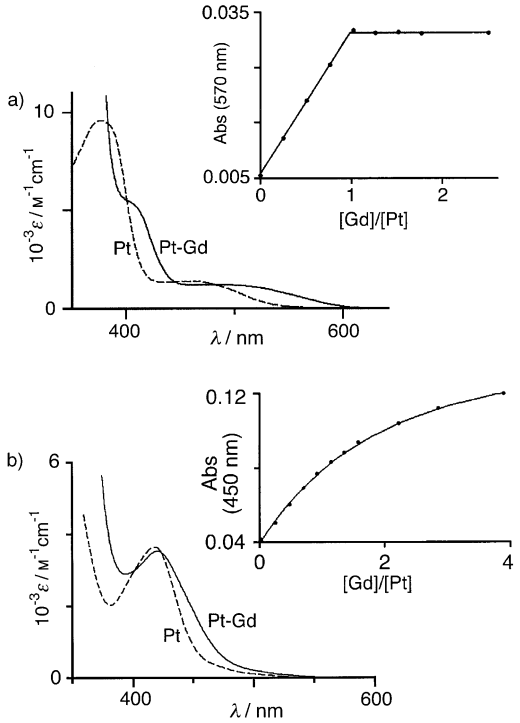

Figure 4. a) Electronic spectra of $[(PPh_3)_2Pt(pdo)]$ (dashed line) and Gd(**A**) (solid line), including (inset) the results of a spectrophotometric titration in which $[Gd(tta)_3(H_2O)_2]$ was added to a 7.4×10^{-5} M solution of $[(PPh_3)_2Pt(pdo)]$ in CH_2Cl_2; b) Electronic spectra of $[Cl_2Pt(dppz)]$ (dashed line) and Gd(**C**) (solid line), including (inset) the results of a spectrophotometric titration in which $[Gd(btfa)_3(H_2O)_2]$ is added to a 4.64×10^{-5} M solution of $[Cl_2Pt(dppz)]$ in CH_2Cl_2.

energy absorption maximum at 460 nm ($\varepsilon = 1400$ M^{-1}cm^{-1}).[17] In the dinuclear series **A** complexes this is red-shifted to 485 nm ($\varepsilon = 1200$ M^{-1}cm^{-1}) and also develops a low-energy tail, which does not decay until about 650 nm; this results in the colour becoming a much deeper brown. Absorptions in the 400–500 nm region are characteristic of $[(PPh_3)_2Pt(OO)]$ complexes (in which "OO" denotes a dianionic *o*-catecholate-type donor).[21] Although these spectra have not been analysed in detail, the transitions have been assigned as a combination of catecholate → phosphine LLCT (ligand–ligand charge transfer) and catecholate → Pt LMCT (ligand–metal charge transfer);[22] some Pt-centred d–d character is also possible. The structural integrity of the series **A** complexes in CH_2Cl_2 was confirmed by a UV-visible spectroscopic titration, in which portions of $[Gd(tta)_3(H_2O)_2]$ were added to a 7.4×10^{-5} M solution of $[(PPh_3)_2Pt(pdo)]$. A graph of absorbance at 550 nm versus the amount of added $[Gd(tta)_3(H_2O)_2]$ (Figure 4a) was linear until one equivalent was added, with no further change thereafter; this implies that the association between the $[(PPh_3)_2Pt(pdo)]$ and $\{Gd(tta)_3\}$ units is at the strong limit at this concentration, that is, $K \gg 1.4 \times 10^4$ M^{-1}. In practice association constants of up to about 10^6 M^{-1} can be measured this way as a reasonable degree of curvature in the titration plot occurs, so the association constant for formation of Gd(**A**) will be greater than this, in agreement with the known association constants of ligands such as bpy and phen.[19c]

The absorption spectrum of mononuclear $[Cl_2Pt(dppz)]$ in CH_2Cl_2 has a maximum at 418 nm ($\varepsilon = 4000$ M^{-1} cm^{-1}), which has been assigned as a $d\pi(Pt) \rightarrow \pi^*(dppz)$ MLCT transition.[18] On addition of portions of $[Gd(btfa)_3(H_2O)_2]$, that is, to generate Gd(**C**), this transition becomes red-shifted slightly to 424 nm and is also broadened, with a substantially increased absorbance between 430 nm and 500 nm relative to that of mononuclear $[Cl_2Pt(dppz)]$ (Figure 4b). The red-shift may be ascribed to the lowering in energy of the dppz π^*-level on coordination of the electropositive lanthanide fragment to the second binding site. By using a 4.64×10^{-5} M solution of $[Cl_2Pt(dppz)]$ in CH_2Cl_2, a graph of absorbance at 450 nm versus the amount of added $[Gd(btfa)_3(H_2O)_2]$ gives a smooth curve that fits well to a 1:1 binding isotherm yielding $K = 1.7 \times 10^4$ M^{-1} (see inset to Figure 4b). This association constant is lower than that obtained by using bpy or phen and may be ascribed to the relatively low basicity of the pyrazine unit relative to pyridine; however, is still high enough to ensure that the complexes remain largely associated at the concentrations used for photophysical studies (see later). The poor solubility of the series **B** complexes precluded a titration of this sort, as the adduct precipitated during the procedure; however, since the only difference is the substituent on the terminal diketonate ligand (thienyl in place of phenyl), it is reasonable to assume that the association constants for the series **B** complexes are comparable to those for the **C** series.

Photophysical studies: The luminescence spectra and emission lifetimes were measured for the Yb, Nd and Er complexes of each series, both in the solid state and in CH_2Cl_2, by using excitation wavelengths of 520 nm for the series **A** complexes, and 440 nm for the series **B** and **C** complexes (Figure 5). Importantly, the $\{Ln(tta)_3\}$ and $\{Ln(btfa)_3\}$ units do not have strong absorptions at wavelengths longer than 400 nm, only very the weak f–f transitions, so use of an excitation wavelength longer than this will result in essentially selective excitation of the Pt-based chromophore. The poor solubility of the series **B** complexes in CH_2Cl_2 meant that a solution lifetime could only be determined for the Yb complex, which is the most strongly emitting of the three; however, solid-state emission lifetimes were determined for all complexes. The results are summarised in Table 3; representative emission spectral profiles and time-resolved decays are shown in Figure 5.

Excitation of the series **A** complexes at 520 nm, into the absorption band of the Pt-based chromophore, produced in every case the NIR emission characteristic of these lanthanide ions, with lifetimes on the microsecond timescale comparable to those of other NIR-emitting complexes for which excitation through a directly coordinated ligand is used.[2–7] This clearly confirms that the Pt chromophore can act as a sensitiser of lanthanide luminescence in the same way as do directly coordinated ligands, following energy transfer from the Pt-centred chromophore to the emissive excited state of the lanthanide ion. The luminescence lifetimes are similar in both the solid state and in solution, confirming the integrity of these complexes in solution (in agreement with the high association constant determined from spectroscopic titrations).

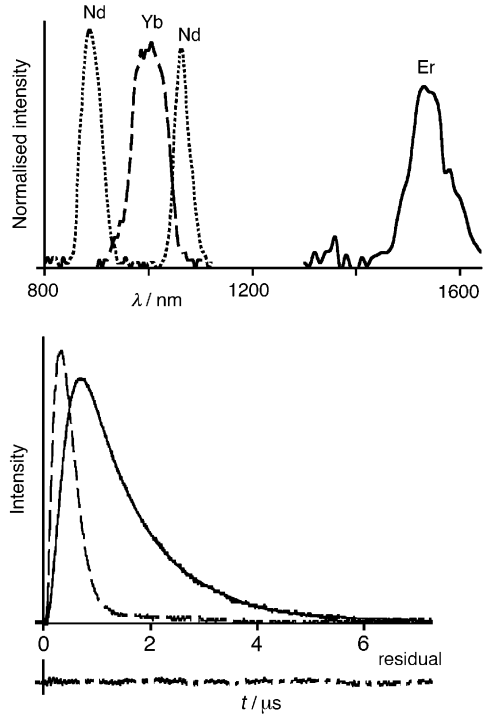

Figure 5. Top: Emission spectral profiles of Er(**A**), Yb(**A**) and Nd(**A**) (the transitions are $^4I_{13/2} \rightarrow {}^4I_{15/2}$ for Er^{III}; $^2F_{5/2} \rightarrow {}^2F_{7/2}$ for Yb^{III}; and $^4F_{3/2} \rightarrow {}^4I_{9/2}$ and $^4F_{3/2} \rightarrow {}^4I_{11/2}$ for the high- and low-energy Nd^{III} emission lines respectively). Bottom: Time-resolved decay of solid Nd(**A**) measured at 1055 nm using excitation at 440 nm. The dashed line shows the detector response, while the solid line shows the observed signal and the fit obtained by reconvolution of the detector response with a single exponential decay component ($\tau = 0.95$ μs). These lines superimpose almost exactly; the residual is shown as alternating dots and dashes, and is offset for clarity.

Table 3. Luminescence data for the complexes.

	τ [μs]		ϕ_{Ln} [a]
	CH_2Cl_2	solid	
Nd(**A**)[b]	0.99	0.95	4×10^{-3}
Yb(**A**)[b]	10.6	11.0	5.3×10^{-3}
Er(**A**)[b]	2.52	1.56	1.8×10^{-4}
Nd(**B**)[c]	weak	0.94	–
Yb(**B**)[c]	7.30	11.5	3.7×10^{-3}
Er(**B**)[c]	weak	1.59	–
Nd(**C**)[c]	0.82	1.02	3.3×10^{-3}
Yb(**C**)[c]	9.50	11.0	4.8×10^{-3}
Er(**C**)[c]	1.50	1.41	1.1×10^{-4}
$[Nd(btfa)_3(H_2O)_2]$[d]	0.15	0.068	6×10^{-4}
$[Yb(btfa)_3(H_2O)_2]$[d]	0.75	0.40	3.8×10^{-4}
$[Er(btfa)_3(H_2O)_2]$[d]	0.29	0.14	2.1×10^{-5}

[a] Quantum yield for metal-based emission process in CH_2Cl_2 determined from $\phi_{Ln} = \tau_{obs}/\tau_0$ (see main text). Emission lifetimes were measured at the following wavelengths: Nd complexes: 1055 nm; Yb complexes: 980 nm; Er complexes: 1530 nm. Data for the $[Ln(tta)_3(H_2O)_2]$ complexes may be found in reference [4]. [b] Excitation at 520 nm. [c] Excitation at 440 nm. [d] Excitation at 337 nm.

The series **B** and **C** complexes differ only in the substituents on the terminal diketonate ligands, as described above. Excitation into the MLCT transition of the Pt^{II}–diimine unit at 440 nm likewise resulted in sensitised NIR emission from the lanthanides at their characteristic wavelengths, implying that d → f energy transfer has occurred. The luminescence lifetimes of the series **B** and **C** complexes are similar to one another and also comparable to those of the corresponding series **A** complexes; this is reasonable given the similarity of the lanthanide luminophore in each case and the relative insensitivity of f-orbitals to the environment provided by the ligands.

In every case the emission lifetimes are considerably longer than those of the parent $[Ln(dik)_3(H_2O)_2]$ complexes determined by excitation at 337 nm (included in Table 3 for comparison), because of the replacement of two water ligands—containing four potentially quenching O–H oscillators—by the N,N-bidentate site of the bridging ligand, in which most of the CH oscillators (which can also act as quenchers, especially for Nd^{III})[3a, 6i] are more remote from the metal centre. The quantum yield values in Table 3 are estimated from Equation (2), in which τ_{obs} is the observed emission lifetime and τ_0 is the radiative or "natural" lifetime, namely, 14, 2 and 0.25 ms for Er^{III}, Yb^{III} and Nd^{III}, respectively;[2a, 3a] these values, therefore, refer only to the quantum yield of the lanthanide-based emission process and take no account of factors such as intersystem crossing and energy-transfer processes.

$$\Phi_{Ln} = \tau_{obs}/\tau_0 \quad (2)$$

The rise-time for the luminescence is in every case within the envelope of the laser pulse (< 5 ns), indicating that energy transfer from the Pt-centred excited state is fast, with a rate of $> 2 \times 10^8\ s^{-1}$ (see example in Figure 5).

Comments on the energy-transfer process: Energy transfer to lanthanide centres is generally considered to occur from the lowest triplet excited state of the sensitiser,[23] implying a Dexter (double electron exchange) mechanism.[24] This requires orbital overlap between donor and acceptor components,[24] which is not a problem when the donor is a directly coordinated ligand chromophore; however, as soon as there is a saturated linker separating the two components, energy transfer becomes slow and may not compete efficiently with the intrinsic deactivation of the donor chromophore.[12] For this reason a short, conjugated connector between antenna (here, the d-block component) and the lanthanide emitter is desirable, as in the complexes described in this paper. In some cases, however, there is good evidence to show that energy transfer can occur by the Förster (dipole–dipole) process,[14, 25] which occurs through-space. In either case, the energy transfer is facilitated by a good matching of donor and acceptor energy levels, subject to the restrictions that 1) the gradient for forward energy transfer is sufficient to prevent back-transfer of energy,[23d] and 2) the relevant selection rules are obeyed; these are $|\Delta J| = 0, 1$ for Dexter energy transfer (with the special case of $J = J' = 0$ being excluded) and $|\Delta J| = 2, 4, 6$ for Förster energy transfer.[23b]

In the complexes described in this paper the energy of the donor state on the Pt^{II} centres is not known, as neither $[(PPh_3)_2Pt(pdo)]$ nor $[Cl_2Pt(dppz)]$ gives rise to luminescence (the solid-state luminescence of $[Cl_2Pt(dppz)]$ is ascribed to a metal–metal interaction that disappears in solution).[18]

However, based on the typical Stokes shifts for other luminescent Pt^{II} complexes (anything from 2000–10000 cm^{-1}, depending on the nature of excited state involved)[18, 26] it is likely that the triplet excited state energies of the $[(PPh_3)_2Pt(pdo)]$ or $[Cl_2Pt(dppz)]$ chromophores in our complexes are at the middle-to-low energy region of the visible spectrum, based on the positions of their absorption maxima.

Nd^{III} has numerous electronically excited states that would be energetically appropriate for sensitisation by the Pt^{II} chromophores, excitation to which is allowed by one or other of the selection rules (e.g., $^4F_{5/2}$, $^2H_{9/2}$, $^4F_{7/2}$ and $^4F_{9/2}$ lie between ca. 13000 and 15000 cm^{-1} and have $\Delta J = 2, 0, 1$ and 0, respectively, from the $^4I_{9/2}$ ground state). For Er^{III} the $^4I_{11/2}$, $^4I_{9/2}$ and $^4F_{9/2}$ levels (lying between 10000 and 16000 cm^{-1}) would be energetically appropriate, although population of only the first of these is allowed by the Förster mechanism ($\Delta J = 2$ with respect to the $^4I_{15/2}$ ground state). Dexter energy transfer is allowed only to the low-lying $^4I_{13/2}$ level ($\Delta J = 1$ from the ground state) at 6500 cm^{-1}, for which the energy-transfer rate would be very slow, because of the large gap between donor and acceptor energy levels. However, Reinhard and Güdel pointed out that energy transfer can involve vibrational as well as electronic excitation of the acceptor chromophore ("phonon-assisted energy-transfer");[27] this is quite reasonable when one considers that coordinated water effectively quenches luminescence from Tb^{III} and Eu^{III} by energy transfer to a highly vibrationally excited state of the O–H oscillators. Accordingly, triplet-mediated energy transfer could occur even when there is no direct overlap between the donor and acceptor levels, provided the acceptor chromophore has vibrational modes available that can also be excited; this is likely when organic ligands are present (as here).

Yb^{III} is a more unusual case as it has only a single excited state, $^2F_{5/2}$, which is 10200 cm^{-1} above the ground state. Direct sensitisation of this excited state (necessarily by the Dexter mechanism, since $\Delta J = 1$ with respect to the $^2F_{7/2}$ ground state) would require the energy-donor state of the Pt^{II} chromophore to have a low-energy tail that has significant intensity in the near-IR region to provide the necessary spectral overlap; alternatively, the phonon-assisted energy-transfer mechanism mentioned above could be invoked.

Conclusion

In conclusion, the rapid and facile formation of adducts between $\{Ln(dik)_3\}$ units and diimine ligands provides a basis for the straightforward preparation of a wide range of heterodinuclear complexes, in which strongly absorbing d-block "complex ligands" with a vacant peripheral binding site are attached to $\{Ln(dik)_3\}$ units. In principle a very wide variety of d-block chromophore/lanthanide emitter dyads is possible based on simple bridging ligands of the type illustrated in this paper, such that the excitation wavelength used to stimulate the luminescence can be tuned throughout the visible region by choice of the appropriate d-block component.

Experimental Section

Materials and methods: The following reagents were prepared according to the literature methods: $[(PPh_3)_2Pt(pdo)]$,[17] $[Cl_2Pt(dppz)]$,[18] $[Ln(btfa)_3(H_2O)_2]$[28] and $[Ln(tta)_3(H_2O)_2]$.[28] UV/Vis spectroscopic titrations were carried out as described previously,[4] by using software provided by Prof. C. Hunter of the University of Sheffield to determine association constants where appropriate.[29] Photophysical studies (steady-state and time-resolved luminescence on solution and solid-state samples) were carried out by using instrumentation and methods described previously.[4] All time-resolved luminescence decay measurements could be satisfactorily fitted to a single-exponential decay.

Syntheses of series A complexes: A mixture of $[(PPh_3)_2Pt(pdo)]$ (34 mg, 37 μmol) and the appropriate $[Ln(tta)_3(H_2O)_2]$ (37 μmol) in benzene/heptane (4:1, v/v; 15 cm^3) was allowed to slowly evaporate over several days. Dark brown-red crystals formed, which were filtered off, washed with hexane and dried to give the Ln(**A**) complexes in 70–85% yield. The complexes are stable to air and moisture. Satisfactory analytical data were obtained (see Table 4). UV/Vis data for La(**A**): λ_{max} ($10^{-3}\varepsilon$) = 486 (1.2), 341 (66), 315 (53), 276 nm (68 $M^{-1}cm^{-1}$).

Table 4. Yield and analytical data for the new complexes

	Yield [%]	Elemental analysis[a]		
		% C	% H	% N
La(**A**)	84	49.8 (49.9)	2.6 (2.8)	1.7 (1.6)
Nd(**A**)	80	49.9 (49.9)	2.7 (2.8)	1.8 (1.6)
Gd(**A**)	75	49.3 (49.4)	2.6 (2.8)	1.6 (1.6)
Er(**A**)	73	49.5 (49.1)	2.6 (2.8)	1.7 (1.6)
Yb(**A**)	72	49.3 (49.0)	2.5 (2.7)	1.7 (1.6)
Nd(**B**)	69	34.2 (34.8)	1.5 (1.7)	4.1 (4.3)
Gd(**B**)	67	34.7 (34.6)	1.7 (1.7)	4.2 (4.2)
Er(**B**)	78	34.3 (34.3)	1.7 (1.7)	4.3 (4.2)
Yb(**B**)	83	34.1 (34.1)	1.3 (1.7)	3.9 (4.2)
Nd(**C**)	70	41.5 (41.0)	2.4 (2.2)	4.4 (4.3)
Er(**C**)	72	40.8 (40.3)	2.1 (2.1)	4.3 (4.3)
Yb(**C**)	61	40.6 (40.1)	2.2 (2.1)	4.3 (4.3)

[a] Calculated values in parentheses.

Syntheses of series B complexes: In a similar manner to the series **A** complexes (above), the series **B** complexes were prepared by slow (several days) evaporation of a mixed CH_2Cl_2/hexane solution (7:1 v/v, 15 cm^3) containing $[Cl_2Pt(dppz)]$ and $[Ln(tta)_3(H_2O)_2]$ in a 1:1 molar ratio, typically 50 μmol of each. Bright red crystals of the dinuclear complexes Ln(**B**) formed; these were collected by filtration, washed with a small amount of CH_2Cl_2 and then a large volume of hexane before drying. Unlike the series **A** and series **C** complexes, these series **B** complexes are only sparingly soluble in CH_2Cl_2. The complexes are stable to air and moisture. Satisfactory analytical data were obtained (see Table 4). UV/Vis data for Gd(**B**): λ_{max} ($10^{-3}\varepsilon$) = 424 (3.5), 341 (60), 277 nm (35 $M^{-1}cm^{-1}$).

Syntheses of series C complexes: A mixture of $[Cl_2Pt(dppz)]$ and $[Ln(btfa)_3(H_2O)_2]$ in a 1:1 molar ratio, typically 50 μmol of each, was dissolved in CH_2Cl_2 to give a clear red solution, which was stirred for 1 h. Reduction in volume on a rotary evaporator resulted in precipitation of the orange/red Ln(**C**) complex, which was filtered off, washed with hexane and dried. The complexes are stable to air and moisture. Satisfactory analytical data were obtained (see Table 4). UV/Vis data for Nd(**C**): λ_{max} ($10^{-3}\varepsilon$) = 424 (3.5), 324 (54), 270 nm (36 $M^{-1}cm^{-1}$).

X-ray crystallography: For each complex a suitable crystal was coated with hydrocarbon oil and attached to the tip of a glass fibre, which was then transferred to a Bruker-AXS SMART (at 173 K) or APEX (at 100 K) diffractometer. Details of the crystal parameters, data collection and refinement for each of the structures are collected in Table 5. After data collection, in each case an empirical absorption correction (SADABS) was applied,[30] and the structures were then solved by conventional direct methods and refined on all F^2 data using the SHELX suite of programs.[31] In all cases, non-hydrogen atoms were refined with anisotropic thermal parameters; hydrogen atoms were included in calculated positions and

Table 5. Crystal, data collection and refinement details for the new crystal structures.

	La(**A**)	Er(**A**)·0.5 C_6H_6	Yb(**A**)	Nd(**B**)·CH_2Cl_2	Nd(**C**)
formula	$C_{72}H_{48}F_9LaN_2O_8P_2PtS_3$	$C_{75}H_{51}ErF_9N_2O_8P_2PtS_3$	$C_{72}H_{48}F_9N_2O_8P_2PtS_3Yb$	$C_{39}H_{24}Cl_4F_9N_4NdPtS_3$	$C_{44}H_{28}Cl_2F_9N_4NdO_6Pt$
M_r	1732.94	1799.65	1766.37	1392.93	1289.93
Diffractometer	Bruker SMART	Bruker APEX	Bruker SMART	Bruker SMART	Bruker APEX
T [K]	173	100	173	173	100
system	triclinic	triclinic	triclinic	monoclinic	monoclinic
space group	$P\bar{1}$	$P\bar{1}$	$P\bar{1}$	$P2_1/c$	$P2_1/c$
a [Å]	15.189(5)	15.202(5)	15.258(8)	12.0819(13)	12.088(4)
b [Å]	16.844(5)	16.665(6)	16.69(2)	24.425(3)	24.657(9)
c [Å]	18.916(6)	18.757(6)	18.581(19)	18.260(2)	18.030(6)
α [°]	86.74(3)	86.22(2)	85.75(4)	90	90
β [°]	69.90(3)	70.360(16)	70.09(3)	98.179(2)	99.06(3)
γ [°]	70.51(2)	69.91(3)	70.39(5)	90	90
V [Å^3]	4275(2)	4156(2)	4188(7)	5333.8(10)	5307(3)
Z	2	2	2	4	4
data/restraints/parameters	14770/0/884	18988/1/911	14344/1/824	12248/14/589	12157/2/570
μ [mm^{-1}]	2.303	2.867	2.958	3.975	3.777
$R1$/w$R2$[a]	0.0843/0.2221	0.0734/0.1895	0.0861/0.2276	0.0693/0.1997	0.0719/0.1677

[a] The value of $R1$ is based on selected data with $I > 2\sigma(I)$; the value of w$R2$ is based on all data.

refined with isotropic thermal parameters which were about 1.2 × (aromatic CH) or 1.5 × (Me) the equivalent isotropic thermal parameters of their parent carbon atoms.

All of the structural determinations were complicated by varying degrees of disorder in lattice solvent molecules, the orientations of the thiophene rings (for the series **A** and **B** structures) and orientations of the CF_3 groups (for the series **A** and **B** structures); this resulted in weak data in every case. Diffuse solvent corrections were used when lattice solvent molecules were so badly disordered that they could not be modelled. For the series **A** complexes, one of the thiophene rings is disordered over two orientations involving a 180° rotation about the bond connecting it to the rest of the ligand, such that the S atom and one of the C atoms exchange positions (e.g., for Er(**A**) the atoms concerned are S(16) and C(19)). These two atom sites were accordingly refined as a mixture of fractional S and C atoms that were constrained to have identical positional and thermal parameters. In Nd(**B**), disorder of one of the thiophene rings again occurred, but the entire thiophene ring could be split into two positions (see main text) with geometric restraints being necessary to keep the geometries of the two components reasonable. In every case the F atoms of the CF_3 groups gave evidence for unresolved rotational disorder and had high thermal parameters. In some cases it was necessary to use isotropic thermal parameters for disordered atoms to keep the refinement stable. In all cases the highest residual electron density peaks were associated with absorption effects (close to a heavy metal atom) or unresolved disorder (close to a CF_3 group).

CCDC 210374–210378 contain the supplementary crystallographic data for this paper. These data can be obtained free of charge via www.ccdc.cam.ac.uk/conts/retrieving.html, or from the Cambridge Crystallographic Data Centre, 12 Union Road, Cambridge CB2 1EZ, UK; fax: (+44)1223–336033; or email: deposit@ccdc.cam.ac.uk.

Acknowledgement

We thank the Royal Society/NATO for a post-doctoral fellowship to N.M.S. and the EPSRC for post-doctoral fellowships to Z.R.B. and S.J.A.P. We are grateful to one of the referees for some helpful suggestions to improve the manuscript.

[1] a) M. P. Bailey, B. F. Rocks, C. Riley, *Analyst* **1984**, *109*, 1449; b) J. Coates, P. G. Sammes, G. Yahioglu, R. M. West, A. J. Garman, *J. Chem. Soc. Chem. Commun.* **1994**, 2311; c) R. R. De Haas, N. P. Verwoerd, M. P. van der Corput, R. P. van Gijlswijk, H. Siitari, H. J. Tanke, *J. Histochem. Cytochem.* **1996**, *44*, 1091; d) M. Montalti, L. Prodi, N. Zaccheroni, L. Charbonniere, L. Douce, R. Ziessel, *J. Am. Chem. Soc.* **2001**, *123*, 12694; e) A. Mayer, S. Neuenhofer, *Angew. Chem.* **1994**, *106*, 1097; *Angew. Chem. Int. Ed. Engl.* **1994**, *33*, 1044; f) A. Beeby, I. M. Clarkson, S. Faulkner, S. W. Botchway, D. Parker, A. W. Parker, J. A. G. Williams, *J. Photochem. Photobiol. B* **2000**, *57*, 83; g) D. Parker, R. S. Dickins, H. Puschmann, C. Crossland, J. A. K. Howard, *Chem. Rev.* **2002**, *102*, 1977; h) "Applications of Coordination Complexes": S. Faulkner, J. L. Matthews in *Comprehensive Coordination Chemistry*, *Vol. 9*, 2nd ed. (Ed.: M. D. Ward), Elsevier, **2003**, in press.

[2] a) S. I. Klink, L. Grave, D. N. Reinhoudt, F. C. J. M. van Veggel, M. H. V. Werts, F. A. J. Geurts, J. W. Hofstraat, *J. Phys. Chem. A* **2000**, *104*, 5457; b) S. I. Klink, G. A. Hebbink, L. Grave, F. C. J. M. van Veggel, D. N. Reinhoudt, L. H. Slooff, A. Polman, J. W. Hofstraat, *J. Appl. Phys.* **1999**, *86*, 1181; c) S. I. Klink, G. A. Hebbink, L. Grave, F. G. A. Peters, F. C. J. M. van Veggel, D. N. Reinhoudt, J. W. Hofstraat, *Eur. J. Org. Chem.* **2000**, 1923.

[3] a) G. A. Hebbink, D. N. Reinhoudt, F. C. J. M. van Veggel, *Eur. J. Org. Chem.* **2001**, 4101; b) G. A. Hebbink, S. I. Klink, L. Grave, P. G. B. Oude Alink, F. C. J. M. van Veggel, *ChemPhysChem* **2002**, *3*, 1014.

[4] N. M. Shavaleev, S. J. A. Pope, Z. R. Bell, S. Faulkner, M. D. Ward, *J. Chem . Soc. Dalton Trans.* **2003**, 808.

[5] a) M. H. V. Werts, J. W. Verhoeven, J. W. Hofstraat, *J. Chem. Soc. Perkin Trans. 2* **2000**, 433; b) M. P. Oude Wolbers, F. C. J. M. van Veggel, F. G. A. Peters, E. S. E. van Beelen, J. W. Hofstraat, F. A. J. Geurts, D. N. Reinhoudt, *Chem. Eur. J.* **1998**, *4*, 772; c) M. H. V. Werts, J. W. Hofstraat, F. A. J. Geurts, J. W. Verhoeven, *Chem. Phys. Lett.* **1997**, *276*, 196; d) J. W. Hofstraat, M. P. Oude Wolbers, F. C. J. M. van Veggel, D. Reinhoudt, M. H. V. Werts, J. W. Verhoeven, *J. Fluoresc.* **1998**, *8*, 301; e) G. A. Hebbink, L. Grave, L. A. Woldering, D. N. Reinhoudt, F. C. J. M. van Veggel, *J. Phys. Chem. A* **2003**, *107*, 2483; f) see reference [3b].

[6] a) M. Asano-Someda, Y. Kaizu, *J. Photochem. Photobiol. A* **2001**, *139*, 161; b) A. I. Voloshin, N. M. Shavaleev, V. P. Kazakov, *J. Lumin.* **2001**, *93*, 115; c) Y. V. Korovin, S. B. Meshkova, N. S. Poluektov, *J. Anal. Chem. USSR* **1984**, *39*, 234; d) Y. Hasegawa, K. Murakoshi, Y. Wada, S.Yanagida, J. H. Kim, N. Nakashima, T. Yamanaka, *Chem. Phys. Lett.* **1996**, *248*, 8; e) W. D. Horrocks, J. P. Bolender, W. D. Smith, R. M. Supkowski, *J. Am. Chem. Soc.* **1997**, *119*, 5972; f) H. Hasegawa, T. Ohkubo, K. Sogabe, Y. Kawamura, Y. Wada, N. Nakashima, S. Yanagida, *Angew. Chem.* **2000**, *112*, 365; *Angew. Chem. Int. Ed.* **2000**, *39*, 357; g) M. Iwamuro, Y. Wada, T. Kitamura, N. Nakashima, S. Yanagida, *Phys. Chem. Chem. Phys.* **2000**, *2*, 2291; h) Y. Wada, T. Okubo, M. Ryo, T. Nakazawa, Y. Hasegawa, S. Yanagida, *J. Am. Chem. Soc.* **2000**, *122*, 8583; i) S. Yanagida, Y. Hasegawa, K. Murakoshi, Y. Wada, N. Nakashima, T. Yamanaka, *Coord. Chem. Rev.* **1998**, *171*, 461.

[7] a) A. Beeby, R. S. Dickins, S. Faulkner, D. Parker, J. A. G. Williams, *Chem. Commun*. **1997**, 1401; b) J. Hall, R. J. Haner, S. Aime, M. Botta, S. Faulkner, D. Parker, J. A. G. Williams, *New J. Chem*. **1998**, *22*, 627; c) S. Faulkner, A. Beeby, R. S. Dickins, D. Parker, J. A. G. Williams, *J. Fluoresc*. **1999**, *9*, 45; d) A. Beeby, S. Faulkner, *Chem. Phys. Lett.* **1997**, *266*, 116; e) A. Beeby, S. Faulkner, D. Parker, J. A. G. Williams, *J. Chem. Soc. Perkin Trans. 2* **2001**, 1268; f) A. Beeby, I. M. Clarkson, R. S. Dickins, S. Faulkner, D. Parker, L. Royle, A. S. de Sousa, J. A. G. Williams, M. Woods, *J. Chem. Soc. Perkin Trans. 2* **1999**, 493; g) A. Beeby, B. P. Burton-Pye, S. Faulkner, J. C. Jeffery, J. A. McCleverty, G. R. Motson, M. D. Ward, *J. Chem. Soc. Dalton Trans.* **2002**, 1923; h) A. Beeby, S. Faulkner, J. A. G. Williams, *J. Chem. Soc. Dalton Trans.* **2002**, 1918.

[8] a) P. Caravan, J. J. Ellison, T. J. McMurry, R. B. Lauffer, *Chem. Rev.* **1999**, *99*, 2293; b) "Applications of Coordination Complexes": E. Tóth, L. Helm and A. Merbach, in *Comprehensive Coordination Chemistry*, *Vol. 9*, 2nd ed. (Ed.: M. D. Ward), Elsevier, **2003**, in press.

[9] a) R. J. Mears,S. R. Baker, *Opt. Quantum Electron.* **1992**, *24*, 517; b) E. Desurvire, *Phys. Today* **1994**, *97*, 20; c) E. Desurvire, *Erbium-Doped Amplifiers. Principles and Applications*, Wiley, New York, **1994**; d) Y. Oshishi, T. Kanamori, Y. Kitagawa, S. Takashashi, E. Snitzer, G. H. Sigel, Jr., *Opt. Lett.* **1991**, *16*, 1747.

[10] N. Sabbatini, M. Guardigli, J.-M. Lehn, *Coord. Chem. Rev.* **1993**, *123*, 201.

[11] a) A. Beeby, R. S. Dickins, S. FitzGerald, L. J. Govenlock, C. L. Maupin, D. Parker, J. P. Riehl, G. Siligardi, J. A. G. Williams, *Chem. Commun.* **2000**, 1183; b) W.-K. Wong, A. Hou, J. Guo, H. He, L. Zhang, W.-Y. Wong, K.-F. Li, K.-W. Cheah, F. Xue, T. C. W. Mak, *J. Chem. Soc. Dalton Trans.* **2001**, 3092

[12] a) S. I. Klink, H. Keizer, F. C. J. M. van Veggel, *Angew. Chem.* **2000**, *112*, 4489; *Angew. Chem. Int. Ed.* **2000**, *39*, 4319; b) S. I. Klink, H. Keizer, H. W. Hofstraat, F. C. J. M. van Veggel, *Synth. Met.* **2002**, *127*, 213.

[13] a) M. Cantuel, G. Bernardinelli, D. Imbert, J.-C. G. Bunzli, G. Hopfgartner, C. Piguet, *J. Chem. Soc. Dalton Trans.* **2002**, 1929; b) M. A. Subhan, T. Suzuki, S. Kaizaki, *J. Chem. Soc. Dalton Trans.* **2002**, 1416.

[14] J.-C. G. Bünzli, C. Piguet, *Chem. Rev.* **2002**, *102*, 1897.

[15] a) N. M. Shavaleev, Z. R. Bell, M. D. Ward, *J. Chem. Soc. Dalton Trans.* **2002**, 3925; b) N. M. Shavaleev, Z. R. Bell, G. Accorsi, M. D. Ward, *Inorg. Chim. Acta*, in press.

[16] N. M. Shavaleev, L. P. Moorcraft, S. J. A. Pope, Z. R. Bell, S. Faulkner, M. D. Ward, *Chem. Commun.* **2003**, 1134.

[17] A. Y. Girgis, Y. S. Sohn, A. L. Balch, *Inorg. Chem.* **1975**, *14*, 2327.

[18] Y.-Y. Ng, C.-M. Che, S.-M. Peng, *New J. Chem.* **1996**, *20*, 781.

[19] a) K. Iftikhar, M. Sayeed, N. Ahmad, *Inorg. Chem.* **1982**, *21*, 80; b) W. H. Watson, R. J. Williams, N. R. Stemple, *J. Inorg. Nucl. Chem.* **1982**, *34*, 501; c) S. Yajima,Y. Hasegawa, *Bull. Chem. Soc. Jpn.* **1998**, *71*, 2825.

[20] a) G. A. Fox, S. Bhattacharya, C. G. Pierpont, *Inorg. Chem.* **1991**, *30*, 2895; b) P. L. Hill, L. Y. Lee, T. R. Younkin, S. D. Orth, L. McElwee-White, *Inorg. Chem.* **1997**, *36*, 5655.

[21] S. Cenini, R. Ugo, G. La Monica, *J. Chem. Soc. A* **1971**, 416.

[22] C. G. Pierpont, C. W. Lange, *Prog. Inorg. Chem.* **1994**, *41*, 331.

[23] a) S. Sato, M. Wada, *Bull. Chem. Soc. Jpn.* **1970**, *43*, 1955; b) G. F. de Sá, O. L. Malta, C. de Mello Donegá, A. M. Simas, R. L. Longo, P. A. Santa-Cruz, E. F. da Silva, Jr., *Coord. Chem. Rev.* **2000**, *196*, 165; c) F. R. Gonçalves e Silva, O. L. Malta, C. Reinhard, H.-U. Güdel, C. Piguet, J. E. Moser, J.-C. G. Bünzli, *J. Phys. Chem. A* **2002**, *106*, 1670; d) M. Latva, H. Takalo, V. M. Mukkala, C. Matachescu, J. C. Rodriguez-Ubis, J. Kankare, *J. Lumin.* **1997**, *75*, 149.

[24] D. L. Dexter, *J. Chem. Phys.* **1953**, *21*, 836.

[25] T. Förster, *Discuss. Faraday Soc*. **1959**, *27*, 7.

[26] a) C. E. Whittle, J. A. Weinstein, M. W. George, K. S. Schanze, *Inorg. Chem.* **2001**, *40*, 4053; b) Q.-Z. Yang, L.-Z. Wu, Z.-X Wu, L.-P. Zhang, C.-H. Tung, *Inorg. Chem.* **2002**, *41*, 5653; c) S. D. Cummings, R. Eisenberg, *J. Am. Chem. Soc.* **1996**, *118*, 1949.

[27] C. Reinhard, H. U. Güdel, *Inorg. Chem.* **2002**, *41*, 1048.

[28] A. I. Voloshin, N. M. Shavaleev, V. P. Kazakov, *J. Lumin.* **2000**, *91*, 49.

[29] A. P. Bisson, C. A. Hunter, J. C. Morales, K. Young, *Chem. Eur. J.* **1998**, *4*, 845.

[30] G. M. Sheldrick, SADABS, A program for absorption correction with the Siemens SMART area-detector system, University of Göttingen, **1996**.

[31] G. M. Sheldrick: SHELXS-97 and SHELXL-97 programs for crystal structure solution and refinement; University of Göttingen, **1997**.

Received: May 13, 2003 [F5132]

